ЖЭТФ, 2024, том 165, вып. 2, стр. 191–195

NON-SEQUENTIAL DOUBLE IONIZATION OF THE ALKALINE EARTH ATOMS WITH A NEAR-SINGLE CYCLE LASER PULSE IN A LINEARLY POLARIZED LASER FIELD

H. Delibašić Marković [a*], ***V. Petrović*** [a], ***I. Petrović*** [b]

[a] *Faculty of Science, University of Kragujevac*
34000 Kragujevac, Serbia

[b] *Academy of Professional Studies Šumadija, Department in Kragujevac*
34000 Kragujevac, Serbia

Received September 25, 2023
revised version September 25, 2023,
Accepted for publication October 4, 2023

Extended Abstract. The full text of this paper is published in the English version of JETP.

DOI: 10.31857/S0044451024020044

Introduction. Over recent decades, the phenomena of multiple ionization events within atoms have been at the forefront of scientific discussion [1–3]. Specifically, nonsequential double ionization (NSDI) occurs when more than one electron is ejected after a single photon absorption, with the process relying on electron-electron correlation. This concept, theoretically proposed, has been validated experimentally for alkaline-earth metals, showing intensity-dependent "knee" shapes in double-ionization yield curves, hinting at electron correlation's significance [4]. This correlation aspect has been neglected by many theorists [5, 6]. NSDI is now crucial in attosecond physics, largely due to the recollision mechanism requiring high-intensity, short-pulse lasers [7]. Within this context, electron dynamics and multi-electron collisions remain focal research points.

Laser field polarization is vital for understanding NSDI. Initial studies focused on linearly polarized laser fields [8], wherein another electron is ejected upon recollision with its parent ion. Circularly polarized fields, however, reduce or negate this recollision [9], though some experiments challenge this [10]. Corkum's rescattering model accounts for this by explaining the absence of nonsequential events in circular polarization [11]. Numerous studies have theorized that NSDI results primarily from electron-electron correlation, specifically through the collective tunneling mechanism [12, 13]. Through tests and simulations [14, 15], the energy of recolliding electrons has been associated with the ponderomotive potential U_p. The semiclassical theory, which combines the adiabatic Landau-Dykhne (LD) approach and classical treatments of subsequent rescattering, provides compelling explanations for atomic NSDI processes [16].

This research introduces an analytical expression for the NSDI transition rate under an intense linearly polarized laser using the LD approach. We delve into the double ionization of alkaline earth atoms across diverse laser intensities. This paper is divided into sections, beginning with this introduction, followed by the main findings, and finally our conclusions.

Theoretical modeling and discussion of results. For years, the two-electron problem puzzled physicists due to its nature as the simplest many-body system where electron interactions matter [17]. When exposed to short-wavelength intense radiation, this system helps explore the relationship between correlation and double ionization. In our work, using a linearly polarized laser field, we derived a formula for the transition rate. This rate describes double ionization in two stages: (i) single photoionization, where electron e_1 interacts with the parent ion, and (ii) recollision phase, where e_1 energizes the bounded electron e_2, leading to potential recollision with the divalent ion. Follow-

* E-mail: hristinadelibasic@pmf.kg.ac.rs

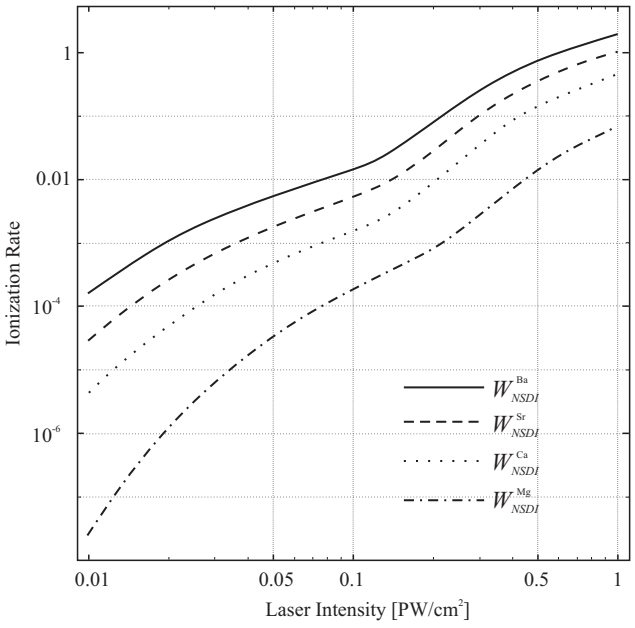

Fig. 1. Intensity dependent NSDI rates for different alkaline-earth metal atoms. The laser's power density ranged from 0.01 $\mathrm{PW/cm^2}$ to 1 $\mathrm{PW/cm^2}$. Solid line is used to represent Ba, dashed line for Sr, dotted line for Ca, and dashed-dotted line for Mg

ing [18], for a system with a time-varying Hamiltonian $H(t)$, the ionization rate, W, between states ψ_i and ψ_f, can be derived using the imaginary part of the classical action as

$$W \propto \exp\left[\, -2\,\mathrm{Im}\{S(\tau)\}\right],$$

where

$$S(\tau) = \int_{t_1}^{\tau} \left[\, E_f(t) - E_i(t)\right]\, dt.$$

It is pivotal to identify the closest complex turning point τ to the real-time axis t, as the roots of the equation $E_f(\tau) = -E_i$ contribute less to the rate formula compared to the nearest one to the real axis.

In the comprehensive exploration of the single photoionization phase, emphasis is placed on the phenomena where the initial electron, denoted e_1, exhibits correlation with its parent ion. This correlation serves as a precursor to the dynamics that unfold in subsequent phases. The context in which this phenomenon is discussed assumes a linearly polarized laser field, described by the equation $F(t) = F\cos\omega t$. One of the pivotal understandings stems from relating the electric fields to the vector potential, $A(t)$. This relationship is epitomized by the equation

$$F(t) = -\frac{1}{c}\frac{\partial A(t)}{\partial t},$$

culminating in the vector potential

$$A(t) = -\frac{\omega}{cF}\sin\omega t.$$

To decipher the nuances of tunneling ionization, one must lean on the revered Landau-Dykhne approach. This approach illuminates the existence of complex turning points in the complex time plane, culminating in the equation $E_f(\tau_1) = -E_i$. This equation carries significant weight, chiefly because it encompasses the energies of the initial and final states. The initial energy, intriguingly, incorporates a term representing electron correlation, derived from previous literature. The culmination of this understanding leads to the depiction of the momentum of expelled photoelectrons as

$$p = \frac{1}{2}\frac{\sqrt{F\eta - 1} - 1}{\eta\sqrt{F\eta - 1}}.$$

Delving further, using the aforementioned energies, we identify the zeros of $E_f(\tau_1) = -E_i$ that reside in the upper half-plane of complex time. This is described by equation

$$\tau_1 = \arcsin\left(\omega\left(p - i\sqrt{2I_p^c}\right)\right)/F + 2\pi c_1,$$

where I_p^c is corrected ionization potential defined as in [19].

Subsequent analyses focus on the temporal integration of the classical turning point relation. This effort culminates in an analytical expression for $S(\tau_1)$ [19]. A notable insight in this context is that at extremely high intensities, certain terms within $S(\tau_1)$ become less consequential, yielding a more concise equation representation. A significant advancement in our investigation was the derivation of the single photoionization rate, W_{SP}. This equation leverages a refined notation of the renowned Keldysh parameter, denoted as

$$\gamma_c = \omega\sqrt{2I_p^c}/F,$$

and is defined as follows:

$$W_{SP} \propto$$

$$\propto \exp\left[-2\left(p^2\gamma_c^3/3\omega + \left(\sqrt{2I_p^c}\right)^3/3F(1-\gamma_c^2/5)\right)\right].$$

In the complex world of atomic interactions, understanding the recollision phase in Nonsequential Double Ionization (NSDI) is paramount. During this phase, the initial electron, e_1, is able to transfer energy to the bound electron e_2. This transfer is contingent upon the kinetic energy of e_1 being less than the ionization

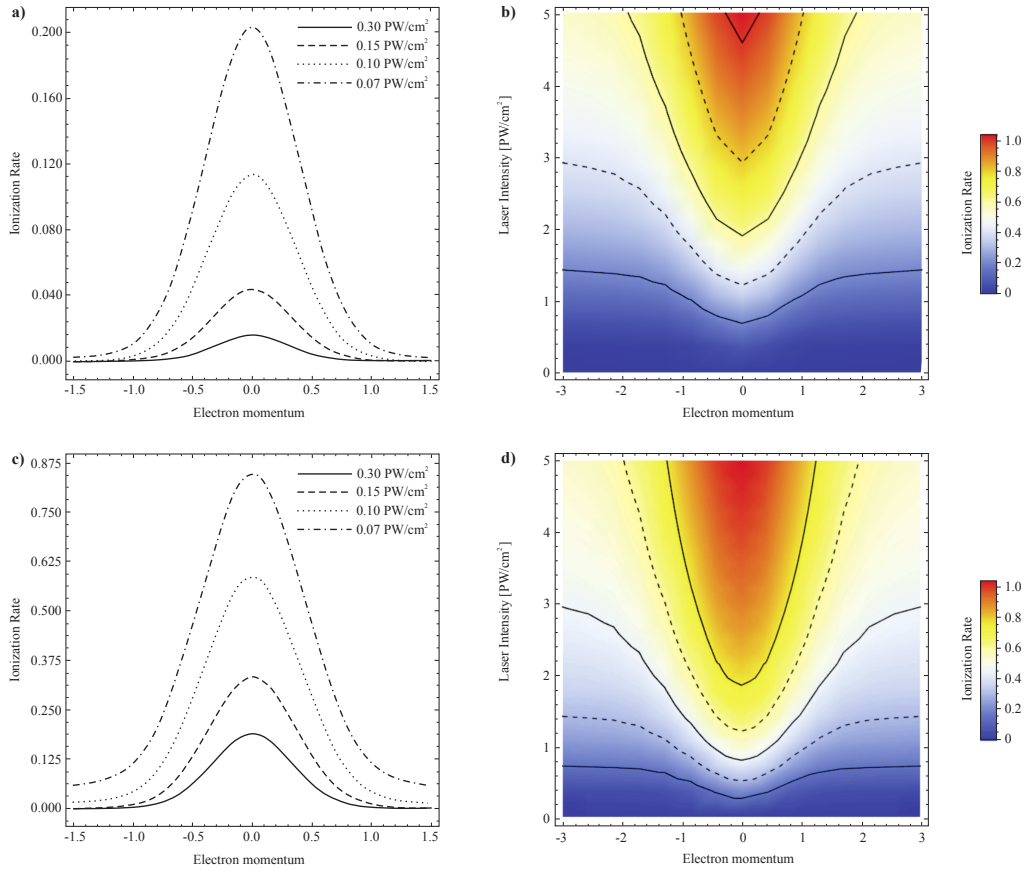

Fig. 2. The momentum distributions of (a), (b) Mg target and (c), (b) Ba target at intensities ranging from 0.3 $\mathrm{PW/cm^2}$ to 0.7 $\mathrm{PW/cm^2}$. The solid lines on the left plots ((a) and (c)) show a laser intensity of 0.3 $\mathrm{PW/cm^2}$, the dashed lines of 0.15 $\mathrm{PW/cm^2}$, the dotted lines of 0.1 $\mathrm{PW/cm^2}$, and the dashed-dotted lines of 0.07 $\mathrm{PW/cm^2}$. The right density plots ((b) and (d)) are the representation of the NSDI ionization rate W_{NSDI} as a function of electron momentum and laser intensity

potential of e_2. Once e_2 undergoes tunneling ionization, it's driven back, influenced by the potent divalent ion, emphasizing the significance of post-tunneling dynamics. Remarkably, the observed probability of NSDI surpasses initial expectations, both experimentally and theoretically, hinting at a rich dynamic beneath the observed phenomena. To gain a clearer mathematical understanding, we determined the energy states for both electrons during the second part of NSDI. Notably, the Coulomb interaction was neglected for the sake of this analysis, simplifying our calculations without compromising the essence of the interaction. Our analytical journey led us to define a complex turning point, τ_2, using the Landau-Dykhne method. This crucial juncture represents a key moment during the recollision phase, shedding light on the underpinnings of the electron interactions. Further mathematical scrutiny, utilizing the Maclaurin series, provided a nuanced expression for this turning point, as well as the classical action $S(\tau_2)$. The culmination of this endeavor was the derivation of the recollision photoionization rate:

$$W_{REC} \propto$$
$$\propto \exp\left[-2\left(p^2\frac{I_{p_2}\gamma_c^2}{4}+\frac{I_p^c\gamma_c}{3\omega}+\frac{1}{5F^2}\left(I_{p_2}-\frac{5}{3I_p^c}\right)\right)\right].$$

The complete NSDI rate, encapsulating both the single photoionization and recollision phases, can be formulated as:

$$W_{NSDI} \propto \exp[-2\,\mathrm{Im}[S(\tau_1)+S(\tau_2)]].$$

This detailed analysis unveils the complex dynamics underlying NSDI, laying a solid groundwork for subsequent research and prospective advancements in the realm of atomic physics.

In examining prior research, it's evident that past studies primarily focused on noble gas atoms. Only recently have fully differential measurements of NSDI on alkaline earth atoms like Mg, Ca, Sr, and Ba been conducted. Despite this, the electron correlation dynamics across various atoms and molecules remain largely

uncharted. Our work employs semiclassical calculations to probe the NSDI physics of Mg, Ca, Sr, and Ba atoms under 800 nm fields and varied laser intensities (0.01–5 PW/cm^2), specifically when the Keldysh parameter $\gamma_c << 1$.

From our results, as illustrated in Fig. 1, it becomes clear that the atomic species plays a critical role in determining the NSDI ionization rates. As the ionization potentials of the atoms increase, there is a discernible reduction in the ionization rates. This suggests that atoms with higher ionization potentials possess an inherent robustness against the external laser field, making them less susceptible to releasing their electrons. When the laser power density surpasses 1 PW/cm^2, a saturation point is reached in the nonsequential contributions, indicating that beyond this intensity, the atoms no longer show a significant increase in ionization activity. Among the studied atoms, Ba stands out as an exception, consistently registering a slightly elevated NSDI probability compared to Sr, Ca, or Mg. This observation not only emphasizes the unique behavior of barium in the context of NSDI but also resonates well with existing experimental findings, as documented in [20].

In Fig. 2, the intricacies of the momentum distributions for Mg and Ba atoms under different laser intensities are laid bare. Contrary to the anticipated double-hump pattern that is typically observed in certain atomic responses, our results showcase a predominant Gaussian-like distribution, with a pronounced peak centering around zero momentum. This intriguing deviation from the expected trend is potentially attributed to the initial simplification where the influence of the Coulomb interactions was not considered [14]. Such an oversight might have resulted in suppressing the subtle structures and patterns that arise due to electron-electron interactions. Furthermore, an intriguing observation from our data is the symmetric nature of these momentum distributions. They not only show symmetry but also exhibit distinct variations as the laser intensity changes, which mirrors the findings of prior research endeavors. Adding another layer to the complexity of these observations is the behavior at lower laser intensities. Here, the momentum density distributions manifest a particularly notable 'plateau' feature that spans between momenta values of -1 au to 1 au. This plateau structure might hint at specific atomic response behaviors or underlying mechanisms at these specific intensities, warranting further investigation.

Summary. In this study, using the LD approach, we formulated a semiclassical model of NSDI, accounting for electron-electron correlation with the assumption that laser radiation is essential for doubly charged ion production. Our results demonstrate a consistent 'knee' structure in NSDI rates across all alkali atoms and a singular peak (Gaussian-like) in momentum distributions. While our model aligns with experimental data for alkaline earth atoms, discrepancies arise in momentum distribution structures when compared to noble gas experiments. The NSDI rates from our model also align closely with those from the ADK theory at higher intensities for the examined targets.

Acknowledgments. This work was supported by the Science Fund of the Republic of Serbia through Program PRISMA - Atoms and (bio)molecules-dynamics and collisional processes on short time scale (ATMOLCOL), Serbian Ministry of Education, Science and Technological Development (Agreement No. 451-03-47/2023-01/200122) and COST Action CA18222 «Attosecond Chemistry».

The full text of this paper is published in the English version of JETP.

REFERENCES

1. Z. X. Lei, Q. Y. Xu, Z. J. Yang, Y. L. He, and J. Guo, Chin. Phys. B. **31**, 063202 (2022).

2. S. L. Haan, L. Breen, A. Karim, and J. H. Eberly, Opt. Express. **15**, 767 (2007).

3. B. HuP, J. Liu, and S. Chen, Phys. Lett. A **236**, 533 (1997).

4. V. V. Suran and I. P. Zapesochny, Sov. Tech. Phys. Lett. **1**, 2 (1975).

5. F. Mauger, C. Chandre, and T. Uzer, J. Phys. B: At. Mol. Opt. Phys. **42**, 165602 (2009).

6. L. Sarkadi, J. Phys. B: At. Mol. Opt. Phys. **53**, 165401 (2020).

7. X. M. Ma, A. H. Tong, Z. Wang, and C. Y. Zhai, Chin. Phys. B. **30**, 123402 (2021).

8. S. Augst, A. Talebpour, S. L. Chin, Y. Beaudoin, and M. Chaker, Phys. Rev. A **52**, R917 (1995).

9. L. B. Fu, G. G. Xin, D. F. Ye, and J. Liu, Phys. Rev. Lett. **108**, (2012).

10. Y. Li, B. Yu, Q. Tang, X. Wang, D. Hua, A. Tong, C. Jiang, G. Ge, Y. Li, and J. Wan, Opt. Express **24**, 6469 (2016).

11. P. B. Corkum, Phys. Rev. Lett **71**(13), 1994 (1993).

12. R. Lafon, J. L. Chaloupka, B. Sheehy, P. M. Paul, P. Agostini, K. C. Kulander, and L. F. DiMauro, Phys. Rev. Lett **86**, 2762 (2001).

13. W. Becker, X. Liu, P. J. Ho, and J. H. Eberly, Rev. Mod. Phys. **84**, 1011 (2012).

14. Y. Liu, S. Tschuch, M. Durr, A. Rudenko, R. Moshammer, J. Ullrich, M. Siegel, and U. Morgner, Opt. Express **15**, 18103 (2007).

15. A. S. Johnson, A. Staudte and D. M. Villeneuve, Chinese J. Phys. **52**, 329 (2014).

16. D. I. Bondar, W. K. Liu, and M. Yu. Ivanov, Phys. Rev. A **79**(2), (2009).

17. X. M. Tong and C. D. Lin, J. Phys. B **38**(15), 2593-2600 (2005).

18. Y. Li, L. Mei, H. Chen, J. Xu, Q. Tang, Y. Zhao, Q. Han, C. Wang, A. Tong, G. Ge, and B. Yu, Int. J. Mod. Phys. B **32**, 1850302 (2018).

19. V. M. Petrovic and T. B. Miladinovic, JETP **122**, 813 (2016).

20. H. P. Kang, S. Chen, W. Chu, J. P. Yao, J. Chen, X. J. Liu, Y. Cheng, and Z. Z. Xu, Opt. Express **28**, 19325 (2020).